PUBLISHED VERSION

Light stop searches at the LHC with monojet events

M. Drees[*]

BCTP and Physics Institute, University of Bonn, Bonn, Germany

M. Hanussek[†]

BCTP and Physics Institute, University of Bonn, Bonn, Germany

J. S. Kim[‡]

Institut für Physik, Technische Universität Dortmund, Dortmund D-44221,
Germany and ARC Centre of Excellence for Particle Physics at the Terascale,
School of Chemistry and Physics, University of Adelaide, Adelaide, Australia

We consider light top squarks (stops) in the minimal supersymmetric Standard Model at the Large Hadron Collider. Here, we assume that the lightest neutralino is the lightest supersymmetric particle (LSP) and the lighter stop is the next-to-LSP. Stop pair production is difficult to probe at the Large Hadron Collider for small stop-LSP mass splitting. It has been shown previously that even in this case stop detection is possible if one considers stop pair production in association with one hard jet. We reconsider this supersymmetric monojet signature and go beyond previous works by including the full Standard Model background and optimizing the cuts, working at the hadron level and including detector effects. As a result, a larger portion of the stop-LSP mass plane becomes accessible to monojet searches.

PACS numbers: 12.60.Jv, 11.30.Pb, 14.80.Ly

I. INTRODUCTION

Supersymmetric extensions of the Standard Model (SM) are popular among the large number of TeV-scale models [1]. In many supersymmetric models, the lightest supersymmetric particle (LSP) is stabilized by employing a discrete symmetry [2]. In the minimal supersymmetric extension of the SM (MSSM), the LSP is the lightest neutralino in large regions of parameter space. Since it escapes detection, the production of two heavier superparticles and their subsequent decays into two LSPs plus several SM particles leads to the famous "missing transverse energy (E_T)" signature for supersymmetry.

This signature has been searched for, most recently by the Large Hadron Collider (LHC) experiments [3]. Unfortunately no signal has yet been found. This allows us to derive quite stringent bounds on the masses of some strongly interacting superparticles. In particular, first generation squarks and gluinos below about 1 TeV are excluded if their masses are roughly equal.

This seems already somewhat high, considering that the main motivation for postulating the existence of superparticles is to stabilize the electroweak (EW) hierarchy against radiative corrections. However, to one loop order essentially only third generation (s)quarks appear in the loop corrections to Higgs mass parameters. Moreover, the analyses published by CMS and ATLAS so far are not sensitive to direct pair production of *only* third generation

squarks, if the other squarks and gluinos are sufficiently heavy [4,5]. One reason is that the cross section for producing a pair of third generation squarks is much smaller than that for producing first generation squarks since no "flavor excitation" contributions exist for third generation squarks. Hence, stop masses of a few hundred GeV are still allowed, and in fact favored by fine-tuning arguments.

In spite of their somewhat smaller production cross sections, the search for the pair production of third generation squarks at the LHC is in principle straightforward, as long as the mass difference to the LSP is sufficiently large. In this case one can employ the usual multijet plus missing E_T [possibly plus one or more lepton(s)] signature; often demanding some of the jets to be tagged as b jets will be helpful [6]. However, if the mass splitting to the LSP becomes small, all SM particles produced in stop decays will become soft, and the missing E_T will therefore also become small. The usual signals will then be swamped by background.

At the same time, there are good reasons to assume that at least the lighter stop mass eigenstate is significantly lighter than the other squarks. First, if supersymmetry breaking is transmitted to the visible sector at some high energy scale, Yukawa contributions to the renormalization group evolution tend to reduce stop masses relative to the masses of first generation squarks [1]. Furthermore, mixing between the $SU(2)$ doublet left (L)-type and $SU(2)$ singlet right (R)-type squarks is proportional to the mass of the corresponding quark, and is therefore most important for top squarks. This mixing will further reduce the mass of the lighter eigenstate (and increase that of the heavier eigenstate).

[*]drees@th.physik.uni-bonn.de
[†]hanussek@th.physik.uni-bonn.de
[‡]jongsoo.kim@tu-dortmund.de

There are also more phenomenological reasons to be interested in quite light stops. One has to do with dark matter. As is well known, the lightest neutralino can be a viable dark matter candidate [1], being weakly interacting and stable (if R parity, or a similar symmetry, is exact). However, for most combinations of parameters the computed LSP relic density is either too large (if the LSP is binolike, which is preferred in many constrained models) or too small (if it is higgsinolike or winolike). One (of several [1]) solutions is to have a binolike neutralino with mass splitting of a few tens of GeV to the lightest stop. In this case coannihilation [7] between these two states can lead to an acceptable relic density [8].

Another reason to consider light top squarks is that in the context of the MSSM they are a necessary condition for EW baryogenesis [9–11]. In fact, a MSSM scenario with a binolike neutralino LSP and a light stop and (higgsinolike) chargino can simultaneously explain the observed baryon asymmetry in the universe and the cosmological dark matter.

However, EW baryogenesis also requires a large CP violating phase in the chargino or neutralino sector. On the other hand, there are severe constraints on the CP phases necessary for EW baryogenesis from electron and neutron electric dipole moment (EDM) bounds [12]. Thus, the phenomenological viable parameter space is strongly constrained. A simple solution is to assume that all other sfermions are very heavy [10,13]. In this case the (lighter) stop may well be the only squark that can be detected by the LHC experiments.

Thus motivated, we study the effects at a hadron collider of a scenario where the lighter stop mass eigenstate $\tilde{t}_1$ is the only strongly interacting light sparticle, with rather small mass splitting to the neutralino LSP. We assume that charginos as well as all other neutralinos are heavier than $\tilde{t}_1$. The dominant sparticle production mechanism is then stop pair production. We further assume that the stop decay channels $\tilde{t}_1 \rightarrow b\tilde{\chi}_1^0 W$ and $\tilde{t}_1 \rightarrow t\tilde{\chi}_1^0$ are kinematically closed and the four-body decay $\tilde{t}_1 \rightarrow \ell\nu_\ell b\tilde{\chi}_1^0$ is strongly phase space suppressed, so that the loop induced two-body decay $\tilde{t}_1 \rightarrow c\tilde{\chi}_1^0$ is the dominant decay mode [14,15].

For sufficiently large mass splitting between the stop and the lightest neutralino, the charm jets become energetic enough to look for a dijet plus missing E_T signature of $\tilde{t}_1$ pair production. The Tevatron experiments were sensitive to mass splitting above 40 GeV [16,17]. Probing stop pair production in this channel becomes difficult for small mass splitting to the LSP, since the collider signature is then given by two very soft charms and correspondingly little transverse missing energy [18]. However, including the effects of (both perturbative and nonpertubative) gluon radiation, $\tilde{t}_1$ pair production should be detectable at e^+e^- colliders even for arbitrarily small mass splitting to the LSP [19]. In fact, LEP2 experiments could rule out $\tilde{t}_1$ masses below 100 GeV [20] even for very small mass splitting.

One possibility to look for light $\tilde{t}_1$ nearly degenerate with the LSP at the LHC is via gluino pair production followed by $\tilde{g} \rightarrow t\tilde{t}_1$ decays [21]. At $\sqrt{s} = 14$ TeV the same-sign top signature should be detectable above the SM background for gluino masses up to 900 GeV. Another possibility [22] is to look for a finite decay length of the light stop produced in gluino decays.

In Ref. [23], an alternative method to discover light stops in the coannihilation region at the LHC was suggested, based on the associate production of a $\tilde{t}_1\tilde{t}_1^*$ pair with a $b\bar{b}$ pair. For relatively light higgsinos, mixed electroweak (EW)-QCD contributions are large and can even exceed the pure QCD prediction since there are $2 \rightarrow 3$ diagrams with an on-shell higgsinolike chargino decaying into a stop and a b jet. These EW contributions are sensitive to the $\tilde{t}_1 - \tilde{\chi}_1^\pm - b$ coupling. Thus, they might be used to test a supersymmetry relation involving superpotential couplings, which has never been addressed so far. However, this requires that the masses of the lighter stop and the lightest neutralino are known, so that the pure QCD contribution, where the $b\bar{b}$ pair originates from gluon splitting, can be subtracted. Determining the stop mass from an independent QCD dominated process would be advantageous for this purpose. Moreover, considering $\mathcal{O}(\alpha_S^3)$ processes might lead to a better discovery reach than the $\mathcal{O}(\alpha_S^2\alpha_W, \alpha_S^4)$ processes contributing to $\tilde{t}_1\tilde{t}_1^+ b\bar{b}$ production.

Therefore, we here reconsider stop pair production in association with a hard jet, which was proposed in Ref. [24]. There it was argued that the soft fragmentation and decay products of the stops cannot be reconstructed as jets for small mass splitting. This inevitably leads to the notion of a monojet [25], i.e. a final state containing a single high momentum jet, whose p_T is mostly balanced by the invisible LSPs, plus some soft particles. In [26] the SM background for monojets was evaluated in the context of searching for extra dimensions; these results were used in [24] to show that the monojet signature from stop pair production can be seen above the SM background up to stop masses of 200 GeV or larger. Stop pair plus photon production were also considered in [24], but due to the reduced cross section the mass reach of this channel is even smaller.

In this work, we will reanalyze stop pair production in association with one hard jet. We perform a signal and background simulation at hadron level. We also simulate the most important detector effects by using a fast detector simulation. In [24] the selection cuts could not be optimized. Here, we develop a set of selection cuts optimized for searching for relatively light $\tilde{t}_1$ squarks nearly degenerate with the neutralino LSP. In addition, we also include $t\bar{t}$ as an important background for the monojet signal, which had been omitted in previous works.

The remainder of this paper is organized as follows. In Sec. II we describe our monojet signal. In Sec. III, we first discuss the dominant background processes and then basic

cuts for a benchmark scenario before presenting our numerical results. We show the discovery reach in the neutralino stop mass plane. We conclude in Sec. IV.

II. STOP PAIR PRODUCTION IN ASSOCIATION WITH A JET AT THE LHC

We consider stop pair production in association with one QCD jet,

$$pp \rightarrow \tilde{t}_1 \tilde{t}_1^* j + X, \qquad (1)$$

where X stands for the rest of the event. We assume that the mass difference between the lightest stop and the lightest neutralino is a few tens of GeV or less, and that the on-shell $\tilde{t}_1 \rightarrow \tilde{\chi}_1^+ b$ and $\tilde{t}_1 \rightarrow b \tilde{\chi}_1^0 W$ decays are closed. Because of the small mass splitting to the LSP, four-body decays like $\tilde{t}_1 \rightarrow \tilde{\chi}_1^0 \ell^+ \nu_\ell b$ are strongly suppressed. However, the flavor changing neutral current stop decay into a charm quark and the lightest neutralino,

$$\tilde{t}_1 \rightarrow c \tilde{\chi}_1^0, \qquad (2)$$

is open. This decay can only occur if $\tilde{t}_1$ has a nonvanishing $\tilde{c}$ component. As pointed out in [14], such a component will be induced radiatively through Cabibbo-Kobayashi-Maskawa mixing even if it is absent at tree level. For simplicity we assume that it has branching ratio of 100%.

The small mass difference to the LSP also implies that both charm "jets" in the signal are rather soft [27]. The charm quarks will then not be useful for suppressing backgrounds since soft jets are ubiquitous at the LHC, and may not be detected as jets at all. Thus our signal will be a single high p_T jet with large missing energy,

$$pp \rightarrow j \not{E}_T, \qquad (3)$$

possibly accompanied by one or more soft jet(s) from gluon radiation and the $\tilde{t}_1$ decay products. At the LHC, the largest contribution to stop pair production in association with a jet comes from gluon fusion diagrams, but contributions from qg and $\bar{q}g$ initial states, which become more important for large $\tilde{t}_1$ masses, are nearly as large [28]. Contributions from $q\bar{q}$ annihilation are relatively small. We perform a full leading order analysis using exact $\mathcal{O}(\alpha_S^3)$ parton-level cross sections for gg, $q\bar{q} \rightarrow \tilde{t}_1 \tilde{t}_1^* g$ and $gq \rightarrow \tilde{t}_1 \tilde{t}_1^* q$.

Since most events have at least one gluon in the initial state, we expect strong QCD bremsstrahlung due to the large color charge. The QCD radiation increases with increasing stop mass. However, the topology of the signal is still simple compared to standard supersymmetric collider signatures: a single energetic jet, which is essentially back-to-back to the missing transverse momentum vector.

III. NUMERICAL ANALYSIS

In this section, we discuss the major backgrounds and describe how to determine them from experimental data, including a discussion of the resulting systematic and statistical errors. Next, we shortly discuss our numerical tools before introducing a specific benchmark scenario. We then show the relevant kinematic distributions and motivate our final cuts. We conclude the section with the discovery reach at the LHC in the neutralino stop mass plane.

A. Backgrounds

The dominant SM backgrounds are:

(i) $Z(\rightarrow \nu\bar{\nu}) + j$ production, i.e. Z boson production in association with a jet. The Z boson decays into a pair of neutrinos. If the charm jets in the signal are very soft, this background looks very similar to our signal. We will see in Sec. III E that $Z(\rightarrow \nu\bar{\nu}) + j$ is the dominant irreducible background after applying all kinematic cuts. Fortunately its size can be directly determined from data: One can measure $Z(\rightarrow \ell^+\ell^-) + j$, where the Z decays into a pair of either electrons or muons. From the known Z branching ratios (BRs) one can then obtain an estimate for the background cross section. However, this procedure will increase the statistical error, since $\mathrm{BR}(Z \rightarrow \ell^+\ell^-) \simeq \mathrm{BR}(Z \rightarrow \nu_i\bar{\nu}_i)/3$ after summing over $\ell = e$, μ and all three generations of neutrinos. Moreover, not all $Z \rightarrow \ell^+\ell^-$ events are reconstructed correctly. Including efficiencies, Ref. [26] estimated that the calibration sample $Z(\rightarrow e^+e^-/\mu^+\mu^-) + j$ is roughly a factor of 5.3 smaller than the $Z(\rightarrow \nu\nu) + j$ background in the signal region [29]. Hence, we expect that the error of this background is $\sqrt{5.3} \simeq 2.3$ times larger than the statistical error.

(ii) $W(\rightarrow \ell\nu) + j$ production, where the W decays leptonically. Unlike the signal, this background contains a charged lepton ($\ell = e^\pm$, $\mu^\pm$), and will thus resemble the signal only if the charged lepton is not identified. This can happen when the charged lepton emerges too close to the beam pipe or (in case of electrons) close to a jet. Since the production cross section for $W(\rightarrow \ell\nu) + j$ is larger than $Z(\rightarrow \nu\bar{\nu}) + j$ by a factor of ~ 3, this will still contribute significantly to the overall background, as we will see in Sec. III E. The $W(\rightarrow \ell\nu_\ell) + j$ background can be determined by extrapolation using events where the lepton is detected.

(iii) $W(\rightarrow \tau\nu) + j$ production, where the W decays into a tau. The reconstructed jets from a hadronically decaying tau are in general not back-to-back in azimuth to the missing momentum vector. Reference [26] exploits this feature to suppress the tau decay channel of $W + j$. However, identification of hadronically decaying τ leptons is not easy. This background can be experimentally determined with the help of $W(\rightarrow \ell\nu) + j$ events where the charged lepton is detected using known tau decay properties. We (quite conservatively)

assign an overall systematic uncertainty of 10% for the total $W + j$ background, including that from $W \to \ell \nu_\ell$ decays.

(iv) $t\bar{t}$ production (including all top decay channels). Top decays will almost always produce two b jets. Since we require large missing E_T, at least one of the W bosons produced in top decay will have to decay leptonically. Note that this again gives rise to a charged lepton (e, μ) or τ, whereas the signal does not contain isolated charged leptons. However, for hadronically decaying τ's, we can have large missing E_T with no e or μ present. This background can again be estimated by normalizing to $t\bar{t}$ events where (at least) one charged lepton is detected. Just as for the $W + j$ background, we assume a total systematic error of 10%.

We consider the above default estimates of systematic errors to be conservative since they do not rely on Monte Carlo simulations. We expect that the SM contribution to the missing transverse energy signal rate will be determined with at least this precision. For example, $W^\pm + j$ and even $\gamma + j$ samples can also be used for reducing the error on the leading $Z(\to \nu\bar{\nu}) + j$ background, since these classes of events have very similar QCD dynamics [30].

In principle, one should also consider single top production, since semileptonic top decays can again give rise to large missing E_T. However, the production cross section for single top production is a factor of $\sim$4 smaller than for $t\bar{t}$. Even though $t\bar{t}$ is important for the cut selection, we will see that in the end it only contributes 5% to the total SM background. For these reasons, we neglect single top production as a background. We do not consider pure QCD dijet and trijet production in our analysis, since a large $\not{E}_T$ cut is expected to essentially remove those backgrounds [31–33]. We also neglect gauge boson pair production as background, since the total cross section is much smaller than that for single gauge boson plus jet production.

There are many SUSY processes leading to a monojet signature, which could be considered to be backgrounds to our signal. LSP pair plus jet production always gives a monojet signature, but has a very small cross section. Associate gluino plus squark production can lead to monojets if the gluino mass is close to that of the neutralino LSP. In addition, squark pair production can give rise to monojets, if both squarks directly decay into the LSP and one of the two jets is lost in the beam direction, or the partons from both squarks are reconstructed in the same jet. Recently, [32] considered squark-wino production. However, as we argued in the introduction, in order to avoid bounds from electron and neutron EDM, we assume that most superparticles are quite heavy. Thus, the production rates of these additional supersymmetric processes are strongly suppressed and we need only consider Standard Model backgrounds.

Estimates for the total hadronic cross sections for these SM backgrounds are given in Table I. The cross section for

TABLE I. Total hadronic cross sections in pb for the main SM backgrounds at $\sqrt{s} = 14$ TeV. The cross sections were calculated with PYTHIA8.150 apart from $t\bar{t}$ production, which is calculated in Ref. [34]. The $V + j(V = W, Z)$ cross sections have been calculated demanding $p_T > 150$ GeV for the parton-level jets.

Process	$Z(\to \nu\bar{\nu}) + j$	$W(\to e\nu_e, \mu\nu_\mu) + j$	$W(\to \tau\nu_\tau) + j$	$t\bar{t}$
σ [pb]	37	94	47	800

the $t\bar{t}$ background has been taken from [34], which includes next to leading order corrections as well as resummation of next-to-leading threshold logarithms. The $W, Z + $ jet backgrounds have been calculated with PYTHIA8.150 [35]. Note that exact $\mathcal{O}(\alpha\alpha_S)$ parton-level cross sections have been used to generate the hardest jet in the $W, Z + $ jet backgrounds. We checked explicitly that using also an exact matrix element for the emission of the second jet and matching to the parton shower does not change the final background estimate (see below).

We have generated $2 \cdot 10^6$ $Z(\to \nu\bar{\nu}) + j$ events, $2 \cdot 10^6$ $W(\to e\nu_e, \mu\nu_\mu) + j$ events, $2 \cdot 10^6$ $W(\to \tau\nu_\tau) + j$ events as well as 10^7 $t\bar{t}$ events.

B. Numerical tools

The masses, couplings and branching ratios of the relevant sparticles are calculated with SPHENO2.2.3 [36], starting from weak-scale inputs for the relevant parameters. We use the CTEQ6L1 parton distribution functions and the one-loop expression for the strong gauge coupling with five active flavors with $\Lambda_{\text{QCD}} = 165$ MeV [37]. Our parton-level signal events are generated with MADGRAPH4.4.5 [38]. These events are then passed on to PYTHIA8.150 [35] for showering and hadronization. As already mentioned, we generate our SM background events directly with PYTHIA8.150 fixing the $t\bar{t}$ normalization as in Table I. Except for the $t\bar{t}$ sample, we employed a parton-level cut of 150 GeV on the minimum transverse momentum of our parton-level jet, which will become the "monojet" in our signal and background; the final cut on the p_T of this jet will be much harder, so that the cut on the parton-level jet, which greatly increases the efficiency of generating signal and background events, does not affect our final results.

In our default treatment only the emission of the first jet in the signal process (1) as well as in the $(W, Z) + $ jet backgrounds have been treated using exact matrix elements. The parton shower is then allowed to produce additional jets whose hardness is limited only by the initial and final state shower scales, for which we adopt the default values. It is known that this does not describe the emission of additional very energetic jets accurately. However, we will see later that we have to reject events containing a second hard jet, and the emission of relatively soft partons should indeed be described adequately by the shower algorithms. In case of the $Z + $ jet background we checked

explicitly that this is indeed the case, by matching $Z + 2$ jet production described by exact matrix elements with the parton shower, using the Michangelo L. Mangano (MLM) matching algorithm [39] (see the Appendix for details).

In case of the $t\bar{t}$ background, only the exact leading order matrix element for the $2 \rightarrow 2$ process has been employed, together with exact matrix elements describing top decay. Since $t\bar{t}$ decay by itself produces between two and six hard partons, there is no need to model the emission of additional hard partons, which will be vetoed anyway, using exact matrix elements. We checked explicitly that $t\bar{t}j$ events generated using exact matrix elements for the emission of the additional parton j with $p_T(j) > 150$ GeV at parton level have an even smaller acceptance after cuts (outlined below) than simple $t\bar{t}$ events.

Finally, in case of the signal, additional jet activity can originate from the charm quarks produced in $\tilde{t}_1$ decays. However, these jets have basically no chance to pass our very stiff cut on the p_T of the hardest jet. We therefore did not generate simple $\tilde{t}_1\tilde{t}_1^*$ pairs without additional parton in the final state. Since our signal estimate is exclusively based on the reaction (1), issues of double counting do not arise.

Our events are stored in the Monte Carlo event record format HEPMC 2.04.01 [40]. We take into account detector effects by using the detector simulation DELPHES1.9 [41], where we choose the default ATLAS-like detector settings. Our event samples are then analyzed with the program package ROOT [42].

We define jets using the anti-k_t algorithm implemented in FASTJET [43], with a cone radius $\Delta R = \sqrt{(\Delta\phi)^2 + (\Delta\eta)^2} = 0.7$, where $\Delta\phi$ and $\Delta\eta$ are the difference in azimuthal angle and rapidity, respectively. All jets have to have $p_T > 20$ GeV. We demand that electrons have $p_T(e) > 10$ GeV and are isolated, i.e. that there is no other charged particle with $p_T > 2.0$ GeV within a cone radius $\Delta R = 0.5$. Since muons can be identified even if they are not isolated and have quite small p_T [44], we include all reconstructed muons with $p_T > 4$ GeV. Note that DELPHES1.9 assumes a track reconstruction efficiency of only 90%, giving a substantial probability that charged leptons are lost. Moreover, we only include true leptons, i.e. we do not attempt to estimate the rate of fake leptons.

In DELPHES1.9, the same object can in principle be reconstructed as several different objects; e.g. an electron can be reconstructed as an electron as well as a jet. Since such double counting of objects has to be prevented, we use an object removal procedure similar to that outlined in Ref. [31]. However, any jet within $\Delta R < 0.2$ of an electron (including nonisolated electrons) will be removed if

$$p_T(\text{jet}) - p_T(e^{\pm}) < 20 \text{ GeV.} \tag{4}$$

This removes "jets" whose energy is dominated by an electron, but we keep hard hadronic jets even if they are very close to an electron. Note that contrary to Ref. [31],

TABLE II. Total hadronic cross sections in pb for the signal at $\sqrt{s} = 14$ TeV. The cross sections were calculated with MADGRAPH4.5.5 with a parton-level cut $p_T > 150$ GeV on the jet.

$m_{\tilde{t}_1}$ [GeV]	120	140	160	180	200	220	240	260	280	300	320
σ [pb]	31	20	13	8.8	6.0	4.2	2.9	2.1	1.5	1.2	0.86

we keep all isolated electrons and all muons even if they are close to a jet.

C. Benchmark scenario

In the Introduction, we motivated scenarios with a light stop and light neutralino in order to be fully consistent with dark matter and electroweak baryogenesis. However, in this study we not only want to discuss these scenarios, but also determine the discovery reach in the stop-neutralino plane where the mass difference between stop and lightest neutralino is at most a few tens of GeV. On the one hand, scenarios with a heavier stop are expected to have a worse signal-to-background ratio than those with a very light stop due to the very quickly decreasing production cross section. However, for heavier stops, producing an additional hard jet reduces the cross section by a smaller factor than for light stops. We choose a scenario with a rather large stop mass in order to probe the discovery reach found in Ref. [24]:

$$m_{\tilde{t}_1} = 220 \text{ GeV,} \tag{5}$$

as a benchmark scenario. The mass of the lightest neutralino is

$$m_{\tilde{\chi}_1^0} = 210 \text{ GeV.} \tag{6}$$

All remaining sparticles are decoupled [45].

We require $p_T(\text{jet}) \geq 150$ GeV for the parton-level jet. The total leading order (LO) cross section for our signal then only depends on the stop mass. The cross section for the benchmark point is $\sigma = 4.2$ pb. We have generated $8 \cdot 10^5$ signal events for our benchmark point. LO predictions for cross sections for different stop masses are listed in Table II.

As described in Sec. II we assume that all $\tilde{t}_1$ undergo two-body decay

$$\tilde{t}_1 \rightarrow c\tilde{\chi}_1^0. \tag{7}$$

We assume that these decays are prompt; a finite impact parameter would greatly facilitate detection of the signal [22].

D. Distributions

In this subsection, we discuss the basic kinematic distributions, and jet and particle multiplicities for the signal as well as for the background processes. The distributions are not stacked on each other and are shown on a logarithmic scale. All distributions are scaled to an integrated luminosity of 100 fb^{-1} at $\sqrt{s} = 14$ TeV at the LHC.
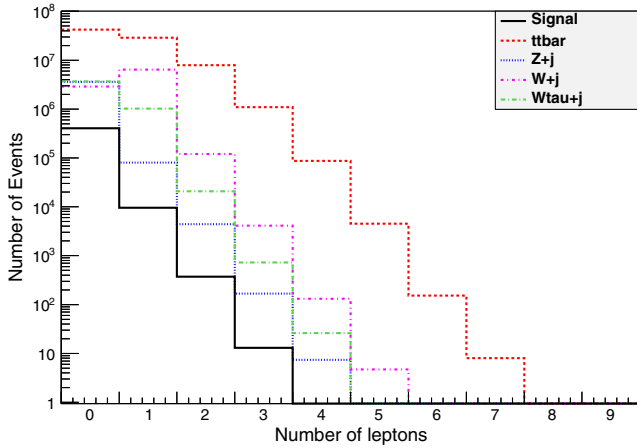
FIG. 1 (color online). Number of leptons for the signal and SM backgrounds assuming an integrated luminosity of 100 fb^{-1} at $\sqrt{s} = 14$ TeV. For the signal we assumed the benchmark scenario of Sec. III C, i.e. $m_{\tilde{\chi}_1^0} = 210$ GeV and $m_{\tilde{t}_1} = 220$ GeV.

FIG. 2 (color online). Number of isolated hadronic taus for the signal and SM backgrounds. Parameters are as in Fig. 1.

We show in Fig. 1 the number of leptons (electrons and muons, as defined in Sec. III B) for signal and background. The signal contains very few charged leptons. In principle, semileptonic $c \to s \ell \nu_\ell$ decays can produce leptons, but these are usually too soft to satisfy our criteria; in addition, most of the remaining electrons are removed by our isolation criterion. The $Z + j$ background also contains very few leptons, since we only consider $Z \to \nu \bar{\nu}$ decays here. In contrast, the $t\bar{t}$ background can have up to seven charged leptons, mostly from semileptonic $t \to b \to c \to s, d$ decays. Note that we include $t\bar{t}$ events where both t quarks decay fully hadronically. This background therefore peaks at $n_\ell = 0$ charged leptons. The $W + j$ background peaks at $n_\ell = 1$ charged lepton; recall that we have only generated $W \to \ell \nu$ decays here, and that we show the $W + j$ background with $W \to \tau \nu_\tau$ separately. In the latter case a charged lepton can arise from the leptonic decays of the tau.

We will later apply a hard cut on missing E_T. This would remove all $W + j$ events where the W decays hadronically, which we therefore did not bother to generate. Similarly, $t\bar{t}$ events can pass this cut only if they contain at least one charged lepton [46]. A veto on charged leptons will therefore efficiently remove most of the SM backgrounds, except for the contribution from $Z(\to \nu \bar{\nu}) + j$.

The distribution of the number of identified taus is shown in Fig. 2. Leptonically decaying taus cannot be reconstructed; they can, however, be vetoed by charged lepton veto if the decay lepton is sufficiently energetic. On the other hand, taus decaying hadronically *can* be identified, although tau identification is not very easy at a hadron collider. In case of hadronic tau decays, only 1-prong events are taken into account for the reconstruction of tau jets in DELPHES where 77% of all hadronically decaying taus are 1-prong events. DELPHES exploits that the cone of tau jets is narrower than that of QCD jets and they state a tau-tagging efficiency of about 30% for $Z \to \tau^+ \tau^-$. We
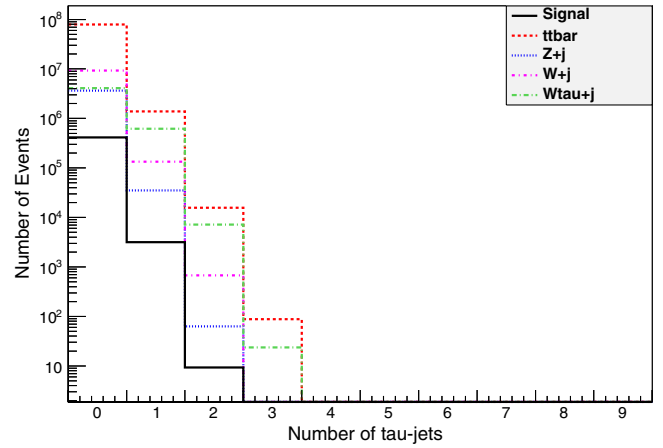
find that the tau-tagging efficiency, as estimated by DELPHES, is much worse for the $t\bar{t}$ background due to the increased hadronic activity. Nevertheless, the $t\bar{t}$ background has the second largest percentage of identified taus, exceeded only by $W(\to \tau \nu) + j$. Even in the latter case only about 25% of all events contain an identified tau, even though *all* of these events do contain a tau lepton [47]. Note that we include mistags of QCD jets as taus, as estimated by DELPHES. In fact, most τ jets identified in the signal are fakes.

Figure 3 shows the number of reconstructed jets including b jets. Jets are reconstructed with the anti–k_t jet algorithm with a cone of $\Delta R = 0.7$. We require the jets to have minimum transverse momentum $p_T > 20$ GeV. We see that the signal distribution has its peak around four jets. Jets can be created not only from the hard interaction (e.g. the jet produced explicitly in the signal as well as in the $V + j$ backgrounds, or the jets produced in top decays), but also from QCD radiation in the initial and/or final state. QCD radiation is controlled by the average partonic squared
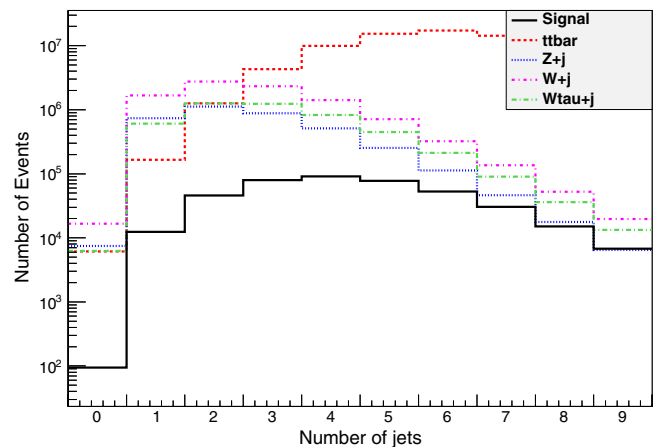

FIG. 3 (color online). Number of jets for the signal and SM backgrounds. Parameters are as in Fig. 1.
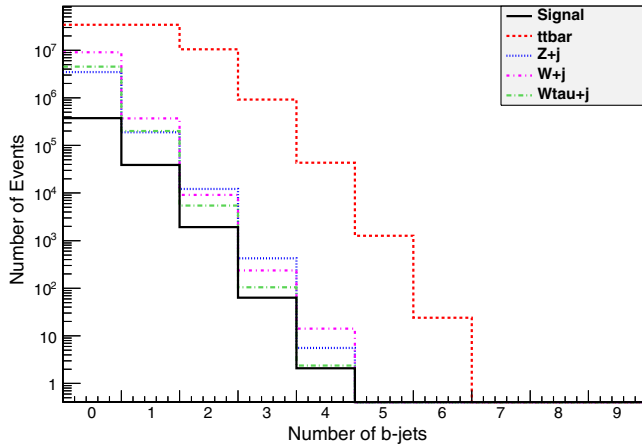
FIG. 4 (color online).   Number of tagged b jets for the signal and SM backgrounds. Parameters are as in Fig. 1.

FIG. 5 (color online). p_T distributions of the hardest jet for the signal and SM backgrounds. Parameters are as in Fig. 1.

center-of-mass energy $\hat{s}$ as well as by the color charges in the initial and final states. As expected from the discussion in Sec. II, we see that the jet multiplicity of the signal is on average larger than for the gauge boson plus jet backgrounds. Not surprisingly, the $t\bar{t}$ background is characterized by the by far largest average jet multiplicity. In previous works, the $t\bar{t}$ background was omitted. Figure 3 indicates that this background can be greatly reduced by cutting against additional jet activity; however, such a cut will reduce the signal more than the $V + j$ backgrounds. Therefore, it is crucial to include the $t\bar{t}$ background in our analysis in order to determine the optimal set of cuts.

Figure 4 shows the number of tagged b jets. A jet is taggable as a b jet if it lies in the acceptance region of the tracking system, i.e. satisfies $|\eta| < 2.5$ in addition to the requirement $p_T > 20$ GeV that all jets have to fulfill, and if it is associated with the parent b quark. DELPHES assumes a tagging efficiency of about 40% for taggable jets; the total b-tagging efficiency is thus less than 40%. DELPHES also assumes mistagging efficiencies of 10% and 1% for charm jets and light-flavored (or gluon) jets, respectively. Not surprisingly, the $t\bar{t}$ background contains the largest number of b tags since every $t\bar{t}$ event contains two b quarks arising from top quark decays, and additional b quarks can emerge from gluon splitting. Unfortunately, the signal contains b tags slightly more often than the $V + j$ backgrounds do. This is partly due to the presence of two c (anti)quarks, which have a relatively high probability to be mistagged as b jets. Moreover, at the parton level the jet in signal events is most often a gluon, which can split into a $b\bar{b}$ pair, whereas in $V + j$ events the parton-level jet is most of the time a quark; signal events are therefore more likely to produce a $b\bar{b}$ pair in the QCD shower. Nevertheless, a b jet veto will suppress the $t\bar{t}$ background with relatively little loss of signal.

The p_T distribution of the hardest jet is given in Fig. 5, where we have also included the b jets. At very large transverse momentum, $p_T(\text{jet}) > 600$ GeV, all curves have similar slopes, since then the hardness of the event
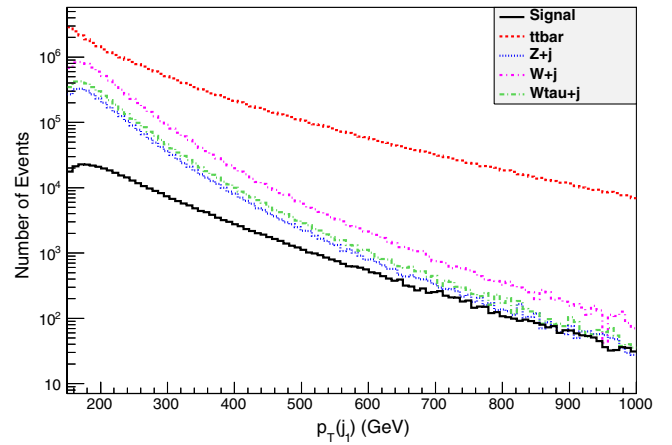
is determined by the p_T of the hardest jet rather than the mass of the produced particles. However, at smaller p_T the $V + j$ backgrounds have a significantly softer spectrum than the signal and the $t\bar{t}$ background; once a pair of massive particles is produced, producing a jet with p_T comparable to, or smaller than, twice the mass of these particles is more likely than in events containing only relatively light particles. Finally, the peaks in the distributions for the signal as well as the $V + j$ backgrounds are due to the parton-level cut of 150 GeV on the jet that is produced as part of the hard partonic collision. Recall that we generated $t\bar{t}$ events without requiring an additional parton, and therefore we did not require a minimum $p_T(\text{jet1})$ here at parton level. As a result, the $t\bar{t}$ contribution peaks at a lower p_T value ($\sim m_t/2$, off the scale shown in Fig. 5) than the other processes. We conclude from Fig. 5 that a lower cut of about 500 GeV on the hardest jet will improve the statistical significance of the signal.

We see in Fig. 6 that the p_T distribution of the second hardest jet is much softer for the signal and the $V + j$
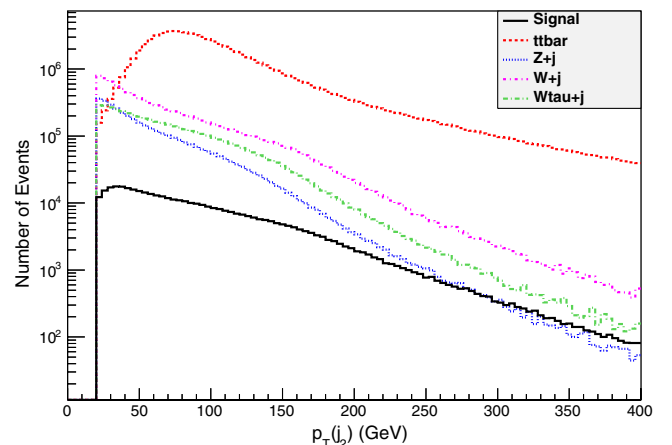

FIG. 6 (color online). p_T distributions of the second hardest jet for the signal and SM backgrounds. Parameters are as in Fig. 1.

backgrounds than that of the hardest jet. Recall that the first jet is generated at parton level with $p_T > 150$ GeV, whereas the second jet comes from QCD showers, or in case of the signal, possibly from stop decays. Both sources give mostly soft jets whose spectrum is backed up against the lower cut of 20 GeV we impose on all jets. In contrast, in $t\bar{t}$ events the hardest and second hardest jet usually both originate from top decay. The p_T spectrum of the second hardest jet therefore peaks not much below that of the hardest jet, at $p_T \simeq 75$ GeV.

From Fig. 3, we have seen that a veto on the second jet is necessary in order to sufficiently suppress the $t\bar{t}$ background. However, if we vetoed all jets with $p_T > 20$ GeV, we would lose too many signal events. We find that it is a good choice to veto all events where the second hardest jet has $p_T > 100$ GeV. We also examined a veto on the third hardest jet with reduced p_T threshold. This would reduce the $t\bar{t}$ background even further. However, it would also remove many signal events and thus a veto on the third jet does not increase the significance of our signal.

Finally, Fig. 7 shows the missing transverse energy distributions of signal and backgrounds. We see that the signal has the slowest falloff. Recall that we did not take into account pure QCD backgrounds such as dijet and trijet events. Thus we need a cut on missing energy in order to suppress these backgrounds [31]. We find that a missing transverse energy cut near 450 GeV maximizes the significance of the signal for our benchmark point. Such a hard cut on the missing E_T, together with the veto on a second hard jet, should suppress the pure QCD background to a negligible level.

E. Discovery potential at the LHC

In the previous subsection, we have discussed the basic distributions which we use to derive a set of kinematical cuts. Now we discuss the statistical significance for our benchmark point. Then, we will show the discovery potential of
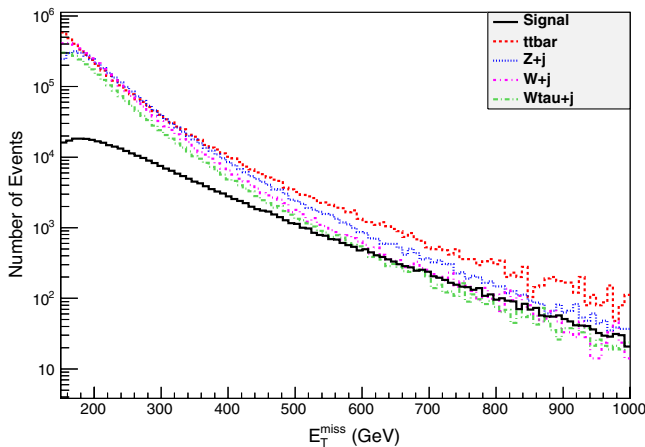

FIG. 7 (color online). Missing transverse energy distributions for the signal and SM backgrounds. Parameters are as in Fig. 1.

our signal in the stop-neutralino mass plane at the LHC for an integrated luminosity of 100 fb^{-1} at $\sqrt{s} = 14$ TeV, using the same set of cuts that optimizes the signal significance for our benchmark point.

As motivated by our discussion in Sec. III D, we apply the following set of cuts:

(i) $p_T(\text{jet}_1) \geq 500$ GeV, i.e. we require one hard jet with $p_T \geq 500$ GeV.

(ii) $\not{E}_T > 450$ GeV, i.e. we demand large missing transverse energy.

(iii) $N_{\text{lepton}} < 1$, i.e. we veto all events with a reconstructed electron or muon with $|\eta| < 2.5$. Recall that we only include isolated electrons with $p_T > 10$ GeV, but all muons with $p_T > 4$ GeV.

(iv) $N_{\text{tau}} < 1$, i.e. we veto all events with an identified tau jet with $|\eta| < 2.5$ and $p_T > 20$ GeV.

(v) $N_{\text{b-jet}} < 1$, i.e. require a veto on all tagged b jets with $p_T > 20$ GeV and $|\eta| < 2.5$.

(vi) $p_T(\text{jet}_2) < 100$ GeV, i.e. we veto the existence of a second hard jet.

The numerical values of the first, second and last cuts have been set by optimizing the signal significance for our benchmark point.

In Table III, we list all cuts in the first column. We display the total number of $(Z \to \nu\bar{\nu}) + j$ (second column), $W(\to \ell\nu_\ell) + j$ (third column), $W(\to \tau\nu_\tau) + j$ (fourth column) and $t\bar{t}$ events (fifth column) for an integrated luminosity of 100 fb^{-1} at the LHC with $\sqrt{s} = 14$ TeV. The signal S, the resulting ratio between signal and background (B) events and the estimate significance $S/\delta B$ are given in the sixth, seventh and eighth column, respectively.

The significance of the signal depends on the error δB (8) of the background. In Sec. III A, we discussed the individual systematical errors. We also mentioned a data driven method to determine the dominant $Z + j$ background from the $Z(\to \ell\ell) + j$ calibration channel. Our overall error estimate is then given by

$$\delta B = \sqrt{5.3 B_{Z+j} + \sum_i B_i + \sum_i (0.1 B_i)^2},$$
$$i = t\bar{t}, W(\to \ell\nu_\ell) + j, W(\to \tau\nu_\tau) + j. \quad (8)$$

We start with a cut on the hardest jet (including b-tagged jets). After applying this cut, $t\bar{t}$ is the dominant background; it is two orders of magnitude larger than the signal and the remaining SM background, as can be seen in the first row of Table III and Fig. 5. Because of the large $t\bar{t}$ background, the signal significance is still very small. Note that for lower stop masses, a less stiff cut on the hardest jet would be slightly more efficient but we optimize our cuts for heavier stops since we would like to determine the discovery reach.

The rather hard cut on the missing transverse energy strongly suppresses the $W + j$ and $t\bar{t}$ backgrounds, but

TABLE III. Cut flow for the benchmark scenario of Sec. III C at the LHC with $\sqrt{s} = 14$ TeV and an integrated luminosity of 100 fb^{-1}. In the second last column, we present the ratio between signal and background number of events. In the last column, we estimate the significance via δB given in Eq. (8).

Cut	$Z(\to \nu\bar{\nu}) + j$	$W(\to e\nu_e, \mu\nu_\mu) + j$	$W(\to \tau\nu_\tau) + j$	$t\bar{t}$	Signal	S/B	$S/\delta B$
$p_T(j_1) > 500$ GeV	27 619	69 802	35 137	2 206 070	17 797	0.008	0.08
$\not{E}_T > 450$ GeV	22 798	20 738	16 835	633 20	13 350	0.108	1.94
Veto on e, μ	22 284	6363	11 978	23 416	12 810	0.200	4.68
Veto on isolated taus	22 221	6274	9031	22 848	12 727	0.21	4.96
Veto on b jets	21 295	5968	8617	11 424	11 064	0.23	6.94
Veto on second jet ($p_T(j_2) \le 100$ GeV)	15 415	3702	5128	1408	5848	0.23	8.17

coming after the hard cut on the p_T of the first jet, has little effect on the signal and on the $Z + j$ background. This holds for relatively small mass splittings between the lighter stop and the lightest neutralino. In these scenarios (including our benchmark scenario), the charm jets are rather soft, leading to large missing transverse energy. As the mass splitting increases, the charm jets become harder and are more often reconstructed, decreasing $\not{E}_T$. We therefore anticipate that the significance of our signal will be worse for larger mass splittings (see below).

As we have shown in Fig. 1, the lepton veto should efficiently reduce the SM background, while having little effect on the signal. We can see in Table III that the leptonic $W + j$ background is reduced by about a factor of 3. $W + j$ events involving leptonically decaying taus from the W are also removed. This cut also reduces the $t\bar{t}$ background significantly. Naively, one would assume that after demanding large missing transverse energy, at least one W boson from $t \to b + W$ or in $W + j$ decays leptonically. However, there is a quite substantial probability that a charged lepton is not reconstructed according to the criteria described in Sec. III B. Finally, the irreducible $Z + j$ background is not affected by this cut.

The tau veto removes 25% of the $W(\to \tau\nu) + j$ background events. However, nearly all $t\bar{t}$ events pass the cut. Requiring a large missing transverse energy cut and a lepton veto should mostly leave $t\bar{t}$ events with one W decaying into a tau. Even so, only a few $t\bar{t}$ events are removed, since the τ tagging efficiency is very poor for $t\bar{t}$ events.

After these four cuts, the signal significance is slightly less than five, with a signal-to-background ratio of 0.21. At this stage $t\bar{t}$ and $Z + j$ are still the dominant backgrounds. The b-jet veto further suppresses the $t\bar{t}$ background by a factor of 2. As expected, it has little effect on the $Z + j$ and $W + j$ backgrounds. We saw in Fig. 4 that a relatively large fraction of the signal events contains a tagged b jet. Thus the veto also removes 13% of the signal events. Nevertheless, this cut increases the signal significance to 6.94.

The final cut vetoing a second hard jet is of crucial importance to further suppress the $t\bar{t}$ background. We now obtain a significance of 8.17 and a rather good signal-to-background ratio of about 0.23. Note that the $t\bar{t}$

background is now quite insignificant, being much smaller than the signal. It could be suppressed even further by reducing the p_T threshold in the second jet veto. However, the number of signal events is decreased more strongly by this veto than the $Z + j$ background, such that our overall significance would get worse.

Searches for monojet signatures by the LHC experiments [48,49] also demand that the transverse momentum vector of the second jet not be close to the missing p_T vector (ATLAS), or equivalently, that the two hardest jets not be back-to-back in the transverse plane (CMS). The ATLAS cut would reduce our signal by about 35%, while the dominant $Z + $ jet background would be reduced by only 12%. The reason is that in case of the signal the visible stop decay products tend to be back-to-back to the hardest jet, making it quite likely that the second hardest jet is also approximately back-to-back with the hardest jet. Such a cut is therefore not beneficial in our case.

The purpose of this cut is to suppress pure QCD multijet backgrounds. However, ATLAS [48] finds that even with quite soft cuts on the hardest jet and the missing E_T, the pure QCD background only amounts to about 5% of the leading $Z + $ jet background *without* such an angular cut. CMS [49] imposes stronger cuts on both the p_T of the hardest jet and the missing E_T. Before the angular cut, the multijet background is about 20% of the $Z + $ jet background. Normally one expects the importance of the pure QCD background to decrease with increasing missing E_T requirement. The fact that the QCD background before the angular cut nevertheless is relatively more important in the CMS analysis might be related to the fact that CMS counts muons as part of the "missing" E_T. Semileptonic c and b decays can therefore generate significantly larger missing E_T as defined by CMS than in the ATLAS definition. Our cut on missing E_T is even harder than the default cut used by CMS (200 GeV), for which the cut flow is shown; as noted above, this should further reduce the relative size of the pure QCD background. Moreover, the CMS "multijet" background is reduced by about factor of 30 by a lepton veto, even though only isolated leptons are vetoed. We conclude from this that our combination of a very stiff missing E_T cut with a lepton veto, which includes

nonisolated muons, should reduce the pure QCD background to a negligible level even without an additional angular cut.

We finally note that the Monte Carlo prediction of the total background *exceeds* the background estimated by CMS directly from the data by about 25% [49]. This gives us some confidence that our background estimate is conservative.

Having discussed the signal significance for our benchmark scenario, we now want to present results for other stop and neutralino masses. As before, we assume that all other sparticles are effectively decoupled. For the sake of simplicity, we apply the same cuts as for the benchmark point, i.e. the cuts in Table III.

In Fig. 8, we present the number of signal events in the stop-neutralino mass plane applying all cuts of Table III. The number of signal events is normalized to a luminosity of 100 fb^{-1} at $\sqrt{s} = 14$ TeV. We see that even after the stiff cuts listed at the beginning of this subsection, our $\mathcal{O}(\alpha_S^3)$ signal process yields in excess of 1000 signal events out to quite large stop masses, as long as the mass splitting to the $\tilde{\chi}_1^0$ is small.

In Fig. 9, we show the statistical significance in the stop-neutralino mass plane for an integrated luminosity of 100 fb^{-1} at $\sqrt{s} = 14$ TeV. We present the discovery reach corresponding to 5σ, 3σ and 2σ, respectively; the latter should be interpreted as the region that can be excluded at 95% C.L. if no signal is found. The stop can dominantly decay into a charm and a neutralino for $m_{\tilde{\chi}_1^0} + m_c < m_{\tilde{t}_1} < m_{\tilde{\chi}_1^0} + m_W + m_b$, the area lying between the two straight
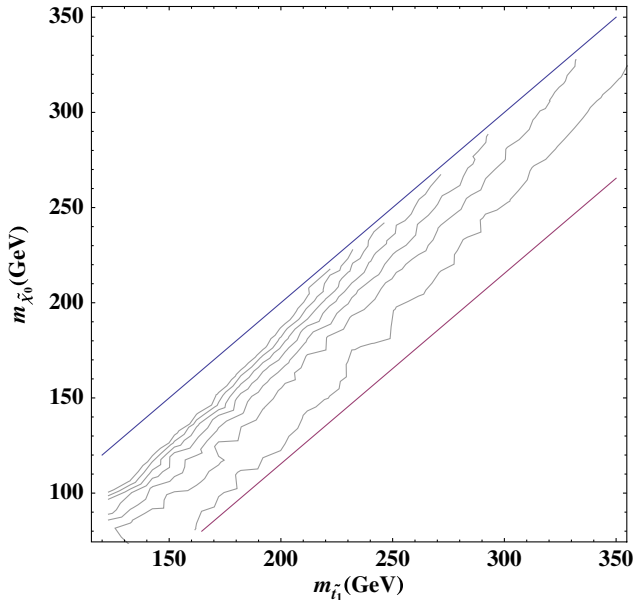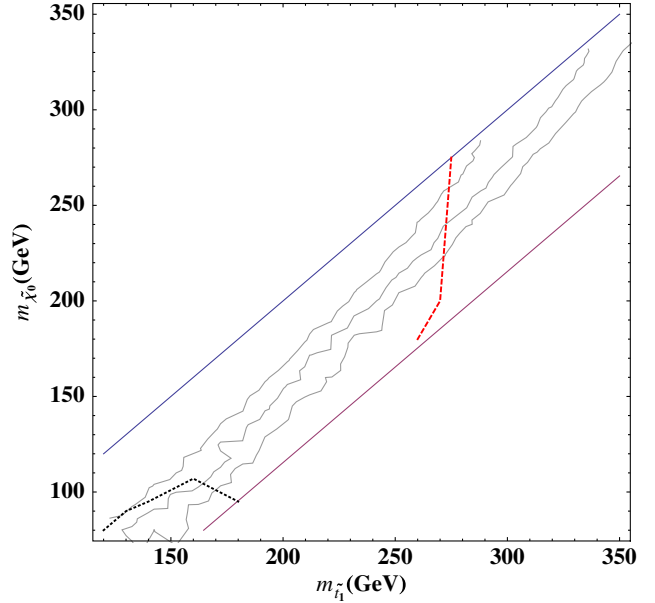

FIG. 9 (color online). Signal significance with background error estimated as in Eq. (8) in the stop-neutralino mass plane assuming an integrated luminosity of 100 fb^{-1} at $\sqrt{s} = 14$ TeV. The two parallel straight lines delineate the region where $\tilde{t}_1 \rightarrow \tilde{\chi}_1^0 c$ decays are allowed but $\tilde{t}_1 \rightarrow \tilde{\chi}_1^0 W^+ \bar{b}$ decays are forbidden. The three grey lines correspond to 5σ, 3σ and 2σ (from top to bottom), respectively. The short-dashed black curve delimits the Tevatron exclusion region, whereas the long-dashed red curve denotes the upper limit of the discovery reach of searches for light stops in events with two b jets and large missing energy.

FIG. 8 (color online). Number of signal events after cuts in the stop-neutralino mass plane assuming an integrated luminosity of 100 fb^{-1} at $\sqrt{s} = 14$ TeV. The two parallel straight lines delineate the region where $\tilde{t}_1 \rightarrow \tilde{\chi}_1^0 c$ decays are allowed but $\tilde{t}_1 \rightarrow \tilde{\chi}_1^0 W^+ \bar{b}$ decays are forbidden. The grey lines correspond to 7000, 6000, 5000, 4000, 3000, 2000 and 1000 signal events (from top to bottom), respectively.

lines in Figs. 9 and 8. The region below the short-dashed black curve is excluded by Tevatron searches at the 95% confidence level [16,17]. In the region to the left of the long-dashed red curve, searches for light stops in events with two b jets and large missing energy [23] should have at least 5σ *statistical* significance.

We see from Fig. 9 that the discovery of stop pairs in association with a jet should be possible for stop masses up to 290 GeV and for mass splittings between stop and neutralino of up to 45 GeV. Stop masses up to 360 GeV can be excluded at 2σ if the mass splitting is very small. As mentioned in the discussion of the missing E_T cut as well as in Ref. [24], the significance of our monojet signal gets worse with increasing mass splitting. Increasing the mass splitting increases the average energy of the c jets. This reduces the missing E_T and increases the probability that the signal fails the veto on a second hard jet. These effects are cumulative: the reduced missing E_T could be compensated by increasing the p_T of the additional parton-level jet. However, this would also increase the p_T of the $\tilde{t}_1 \tilde{t}_1^*$ pair, and hence the average p_T of the c jets from $\tilde{t}_1$ decay.

The region close to the maximal allowed mass splitting (for the assumed loop-level two-body decay of $\tilde{t}_1$) could perhaps be probed through conventional searches for dijet plus missing E_T events without demanding the presence of

an additional parton-level jet. Alternatively one could reduce the missing E_T cut, and try to suppress the $V + j$ backgrounds by a cut on the minimal multiplicity of charged particles [23]. In both cases some sort of c-jet tagging would be helpful and perhaps even crucial. Unfortunately, little is known (to us) about the capabilities of the LHC experiments to detect charm jets (or at least to isolate an event sample enriched in charm jets). We have therefore not attempted this approach here.

The dashed red line in Fig. 9 indicates that the two b jets plus missing transverse energy signature [23] is degraded less for larger mass splittings compared to our monojet signal. There the presence of two hard b jets allowed the use of a much milder missing E_T cut of "only" 200 GeV, and no veto against additional jet activity was used. However, the analysis of [23] is not really comparable to our present work. First of all, only statistical uncertainties were considered in [23], whereas in the present case the uncertainty of the background, and hence the total significance, is dominated by the systematic errors; for example, after all cuts our benchmark point has a *statistical* significance of about 37, compared to our stated significance of "only" 8.17. Secondly, detector effects were not included in [23]. At least according to DELPHES, this overestimates the efficiency of the lepton veto in reducing $W + j$ and top backgrounds. Finally, the red curve shown in Fig. 9 holds under the assumption that there is a higgsinolike chargino just 20 GeV above the $\tilde{t}_1$; this increases the cross section for $\tilde{t}_1 \tilde{t}_1^* b\bar{b}$ production, which receives contributions from $\tilde{t}_1 \tilde{\chi}_1^- \bar{b}$ production followed by $\tilde{\chi}_1^- \to \tilde{t}_1^* b$ decays (as well as charge conjugate processes).

As noted above, the total uncertainty of our background estimate is dominated by the systematic error on the $W + 1$ jet background, which we estimate to be 10%. This is compatible with recent preliminary ATLAS results on monojet searches at the 7 TeV LHC [48,49]. Since with the accumulation of additional data, our understanding of $W + 1$ jet production should improve, we consider this estimate, and the resulting estimate of the LHC reach, to be quite conservative. For example, Ref. [26] estimates the *total* squared uncertainty from all W, $Z + 1$ jet backgrounds to be $7B_{Z+j}$. This would reduce the total uncertainty δB of the background after all cuts from about 715 (our estimate) to about 360, i.e. by a factor of 2. Once the total error on the background has been established, Fig. 8 can be used to determine the region of parameter space that can be probed at a given significance.

Finally, our estimate of the signal S also has uncertainties. Since we define the significance as $S/\delta B$ the systematic (theoretical) uncertainty on S will only change the signal reach appreciably if the uncertainty is sizable. Since we are employing leading order $\mathcal{O}(\alpha_S^3)$ expressions for the parton-level signal cross section, NLO corrections might indeed be sizable. One often attempts to estimate their magnitude by varying the factorization and renormal-

ization scales. For example, for $m_{\tilde{t}_1} = 120$ GeV, setting both of these scales equal to the stop mass increases the parton-level cross section before cuts to 49 pb; this is a factor 1.6 larger than the value of 31 pb we quote in Table II, which has been computed using the MADGRAPH default scale choices. Unfortunately, no NLO calculation of squark pair production with radiation of an additional jet has been performed as yet. All other theoretical uncertainties (due to details of the QCD shower and fragmentation or the choice of parton distribution functions) are significantly smaller than this estimate of the uncertainty due to NLO corrections.

IV. SUMMARY AND CONCLUSION

In this work, we considered light stops nearly degenerate with the lightest neutralino, with mass splitting of at most a few tens of GeV. Including *CP* phases in a sufficiently light electroweak gaugino-higgsino sector can then lead to scenarios consistent with electroweak baryogenesis and provide the right amount of dark matter. However, in such a scenario the direct production of a pair of light stops in stop pair production is difficult to detect at a hadron collider like the LHC since the decay products of the stops are quite soft.

One solution is to examine stop pair production in association with two b jets [23]. This could not only serve as a stop discovery channel; it could also be used to constrain Yukawa couplings of superparticles. The mixed QCD-EW production channels are sensitive to the $\tilde{t}_1 - \tilde{\chi}_1^+ - b$ coupling. However, in order to determine the value of this coupling from future data, it is necessary to know the stop mass so that the QCD contribution can be subtracted.

In Ref. [24] a different process with negligible EW contributions was proposed: stop pair production in association with a hard jet. In this paper we reanalyzed this process with some significant improvements. First, we included the $t\bar{t}$ background, which had been neglected in previous works. Second, we simulated the signal and full SM background with the recent Monte Carlo simulations including a detector simulation. Finally, we optimized the selection cuts, which was not done in Ref. [24].

We discussed all the relevant collider observables for a specific benchmark point with $m_{\tilde{t}_1} = 220$ GeV and $m_{\tilde{\chi}_1^0} = 210$ GeV. This led to a set of optimal cuts. We found that demanding a lot of missing transverse energy ($\not{E}_T \geq 450$ GeV) and large transverse momentum of the hardest jet ($p_T(j_1) \geq 500$ GeV) is not sufficient to see an excess above the SM background. However, additionally imposing a lepton veto and a veto on the second jet ($p_T(j_2) \leq 100$ GeV) is very efficient for background suppression; the remaining dominant background process being the irreducible process $Z(\to \nu\bar{\nu}) + j$. Fortunately, this background can be determined experimentally from $Z(\to \ell\ell) + j$, although with reduced statistics. Here, we adopted a conservative estimate of the background uncertainty of the

$Z(\rightarrow \nu\bar{\nu}) + j$ channel from Ref. [26] using $\delta B_{Z(\rightarrow \nu\bar{\nu})+j} = 5.3 B_{Z(\rightarrow \nu\bar{\nu})+j}$. On the remaining SM backgrounds we assumed a systematic error of 10%. For our benchmark point, we showed that we can have a total signal significance exceeding 8 for an integrated luminosity of 100 fb^{-1} at $\sqrt{s} = 14$ TeV. For the same cuts, we examined the discovery reach in the stop-neutralino mass plane and showed that this process can probe stop masses up to 290 GeV if the mass splitting to the LSP is very small. This is well above the maximal $\tilde{t}_1$ mass compatible with electroweak baryogenesis in the MSSM.

After having reexamined the monojet signature in this work, we are currently investigating the potential of reconstruction the $\tilde{t}_1 - \tilde{\chi}_1^{\pm} - b$ coupling by comparing the monojet channel to the two b jets plus missing energy channel. Moreover, it would be interesting to devise methods to probe light top squarks with somewhat larger mass splitting to the LSP. Considering the importance that top squarks play in naturalness arguments for supersymmetry, this offers a good motivation to our experimental colleagues to investigate charm tagging at the LHC.

ACKNOWLEDGMENTS

APPENDIX: JET PARTON MATCHING

In our work, we have estimated the SM backgrounds to our monojet signal by using the exact leading order matrix elements of the $V + 1$jet ($V = W, Z$) processes where additional partons are emitted via the parton shower. However, it is common lore that a parton shower is only valid in the limit of soft and collinear emissions. Since we apply a (relatively loose) jet veto on the second jet, it should be investigated whether jet matching for the second jet affects our results of the $V + j$ backgrounds, see also the discussion in Sec. III B.

Here, we shortly study the impact of the exact matrix element calculation of single gauge boson production in association with up to two parton final states at the example of the $Z + $jet background. We use the parton-jet MLM matching algorithm [39], which is based on event rejection. The numerical matching is performed with MADGRAPH5.1.4.6 interfaced with the shower generator PYTHIA6.4 where we applied a p_T sorted parton shower. Hadronization is included, but we switch off the underlying event for this study.

TABLE IV. Cut flow for an unmatched $Z + 1j$ sample and a matched $Z + 1j$ and $Z + 2j$ sample. We assumed an integrated luminosity of 100 fb^{-1} at the LHC with $\sqrt{s} = 14$ TeV.

Sample	$p_T(j_1) > 500$ GeV	$\not{E}_T > 450$ GeV	Jet veto
Unmatched	28 048	23 080	16 002
Matched	63 021	31 478	16 387

(It has of course been included in the analysis presented in the main text). We produce a matched sample of $Z + 1$jet and $Z + 2$jet events with subsequent $Z \rightarrow \nu\bar{\nu}$ decays. We demand parton level cuts on the missing transverse energy of $E_T > 150$ GeV and minimum transverse energy cut on the leading jet with $p_T > 150$ GeV. We have chosen a merging scale of $Q = 60$ GeV and kept the remaining default settings in MADGRAPH. We checked that this choice of matching scale leads to smooth distributions, and that our results are stable against small variations of the matching scale. We compare the matched sample with a description very similar to that used in the main text where $Z + 1$ parton events generated with exact matrix elements are interfaced with PYTHIA6.4. Here the second jet arises from the parton shower.

Our numerical results are summarized in Table IV. We present the number of events after applying the relevant kinematic cuts scaled to an integrated luminosity of 100 fb^{-1} at $\sqrt{s} = 14$ GeV for both samples. We start with a p_T cut on the hardest jet. Matching increases the cross section after this first cut by a factor 2.25, as one can see in the second column. The first cut shows that the parton shower description produces a less energetic leading jet than the two-jet matrix element description, although the first jet is exact in both samples. The reason for this is as follows. In the unmatched case, the second jet prefers phase space configurations close to the leading jet. In the matched sample, the second jet tends to be not as strongly centered around the leading jet in phase space, and thus events where the second jet is closer to the Z increase the average p_T of the leading jet.

However, as a consequence of the second jet being closer to the Z on average, the missing transverse momentum distribution becomes softer since the preferred kinematical configuration is determined by minimizing the squared partonic center-of-mass energy $\hat{s}$. Thus matching reduces considerably the efficiency of the missing transverse momentum cut, so that the ratio of cross sections with and without matching is reduced to 1.36. Finally, we find that after imposing the jet veto, both estimates of the cross section agree well because, as expected, the second jet from the exact matrix element is on average harder than the parton shower jet in the unmatched case. In other words, matching increases the number of events with hard second jet, which are in any case rejected by our jet veto. We conclude that the background estimates with and without MLM matching agree well within the statistical uncertainties.

[1] M. Drees, R. M. Godbole, and P. Roy, *Theory and Phenomenology of Sparticles* (World Scientific, Singapore, 2004); H. Baer and X. R. Tata, *Weak Scale Supersymmetry: From Superfields to Scattering Events* (Cambridge University Press, Cambridge, 2006).

[2] L. E. Ibanez and G. G. Ross, Nucl. Phys. **B368**, 3 (1992).

[3] G. Aad *et al.* (ATLAS Collaboration), Phys. Lett. B **710**, 67 (2012); Phys. Rev. D **85**, 012006 (2012); J. High Energy Phys. 11 (2011) 099; S. Chatrchyan *et al.* (CMS Collaboration), J. High Energy Phys. 08 (2011) 156; 08 (2011) 155; Phys. Rev. Lett. **107**, 221804 (2011).

[4] S. Sekmen *et al.*, J. High Energy Phys. 02 (2012) 075; C. Brust, A. Katz, S. Lawrence, and R. Sundrum, J. High Energy Phys. 03 (2012) 103; M. Papucci, J. T. Ruderman, and A. Weiler, arXiv:1110.6926; N. Desai and B. Mukhopadhyaya, J. High Energy Phys. 05 (2012) 057; X.-J. Bi, Q.-S. Yan, and P.-F. Yin, Phys. Rev. D **85**, 035004 (2012).

[5] Very recently ATLAS published [6] an analysis of a search for light sbottom pairs using about 2 fb^{-1} of data, which excludes $\tilde{b}_1$ with mass below 400 GeV if $\tilde{b}_1$ decays with unit branching ratio into the lightest neutralino, assuming the mass of that neutralino is sufficiently small.

[6] G. Aad *et al.* (ATLAS Collaboration), Phys. Rev. Lett. **108**, 181802 (2012).

[7] K. Griest and D. Seckel, Phys. Rev. D **43**, 3191 (1991).

[8] C. Boehm, A. Djouadi, and M. Drees, Phys. Rev. D **62**, 035012 (2000).

[9] P. Huet and A. E. Nelson, Phys. Rev. D **53**, 4578 (1996).

[10] M. Carena, G. Nardini, M. Quiros, and C. E. M. Wagner, Nucl. Phys. **B812**, 243 (2009).

[11] Y. Li, S. Profumo, and M. Ramsey-Musolf, Phys. Lett. B **673**, 95 (2009).

[12] M. J. Ramsey-Musolf and S. Su, Phys. Rep. **456**, 1 (2008); J. R. Ellis, J. S. Lee, and A. Pilaftsis, J. High Energy Phys. 10 (2008) 049; Y. Li, S. Profumo, and M. Ramsey-Musolf, J. High Energy Phys. 08 (2010) 062.

[13] K. Nakamura *et al.* (Particle Data Group), J. Phys. G **37**, 075021 (2010).

[14] K. i. Hikasa and M. Kobayashi, Phys. Rev. D **36**, 724 (1987); M. Mühlleitner and E. Popenda, J. High Energy Phys. 04 (2011) 095.

[15] C. Boehm, A. Djouadi, and Y. Mambrini, Phys. Rev. D **61**, 095006 (2000).

[16] V. M. Abazov *et al.* (D0 Collaboration), Phys. Lett. B **665**, 1 (2008).

[17] CDF Collaboration, CDF Report No. 9834.

[18] C. Balazs, M. S. Carena, and C. E. M. Wagner, Phys. Rev. D **70**, 015007 (2004).

[19] M. Drees and O. J. P. Eboli, Eur. Phys. J. C **10**, 337 (1999).

[20] P. Achard *et al.* (L3 Collaboration), Phys. Lett. B **580**, 37 (2004).

[21] S. Kraml and A. R. Raklev, Phys. Rev. D **73**, 075002 (2006).

[22] G. Hiller, J. S. Kim, and H. Sedello, Phys. Rev. D **80**, 115016 (2009).

[23] S. Bornhauser, M. Drees, S. Grab, and J. S. Kim, Phys. Rev. D **83**, 035008 (2011).

[24] M. Carena, A. Freitas, and C. E. M. Wagner, J. High Energy Phys. 10 (2008) 109.

[25] G. Arnison *et al.* (UA1 Collaboration), Phys. Lett. **139B**, 115 (1984).

[26] L. Vacavant and I. Hinchliffe, arXiv:hep-ex/0005033; J. Phys. G **27**, 1839 (2001).

[27] A tiny fraction of signal events have highly boosted stop squarks producing hard charm jets.

[28] For light stop masses of 120 GeV, the qg contribution is already about 43% of the total cross section. It increases to 47% for 300 GeV stops.

[29] Reference [26] cites a factor of seven between the $Z \to \ell^+\ell^-$ control sample and the *total* background from $V + j$ production ($V = W^\pm$, Z), after applying a lepton veto in the signal. The ratio of 5.3 follows since according to the cuts of [26], about 75% of the $V + j$ background comes from $Z(\to \nu\bar{\nu}) + j$.

[30] H. Ita, Z. Bern, L. J. Dixon, F. F. Cordero, D. A. Kosower, and D. Maitre, Phys. Rev. D **85**, 031501 (2012).

[31] G. Aad *et al.* (ATLAS Collaboration), arXiv:0901.0512.

[32] B. C. Allanach, S. Grab, and H. E. Haber, J. High Energy Phys. 01 (2011) 138; 07 (2011) 087; 09 (2011) 027.

[33] G. Aad *et al.* (ATLAS Collaboration), Report No. ATLAS-CONF-2010-065.

[34] R. Bonciani, S. Catani, M. L. Mangano, and P. Nason, Nucl. Phys. **B529**, 424 (1998); **B803**, 234(E) (2008).

[35] T. Sjostrand, S. Mrenna, and P. Z. Skands, Comput. Phys. Commun. **178**, 852 (2008).

[36] W. Porod, Comput. Phys. Commun. **153**, 275 (2003).

[37] J. Pumplin, D. R. Stump, J. Huston, H. L. Lai, P. M. Nadolsky, and W. K. Tung, J. High Energy Phys. 07 (2002) 012.

[38] F. Maltoni and T. Stelzer, J. High Energy Phys. 02 (2003) 027.

[39] M. L. Mangano, M. Moretti, F. Piccinini, and M. Treccani, J. High Energy Phys. 01 (2007) 013.

[40] M. Dobbs and J. B. Hansen, Comput. Phys. Commun. **134**, 41 (2001).

[41] S. Ovyn, X. Rouby, and V. Lemaitre, arXiv:0903.2225.

[42] R. Brun and F. Rademakers, Nucl. Instrum. Methods Phys. Res., Sect. A **389**, 81 (1997).

[43] M. Cacciari, arXiv:hep-ph/0607071.

[44] S. Franchino (ATLAS Collaboration), arXiv:1111.4928.

[45] In order to reduce stop and sbottom loop contributions to electroweak precision variables, in particular to the ρ parameter [50], our $\tilde{t}_1$ should be predominantly an $SU(2)$ singlet. However, the stop mixing angle and the identity of the LSP are irrelevant for our analysis. Similarly, the presence of relative light higgsino-like chargino and neutralino states, as required for EW baryogenesis, does not affect our analysis, as long as they are not produced in $\tilde{t}_1$ decays.

[46] Since the other top (anti)quark might decay fully hadronically, we cannot simply enforce semileptonic top decays when simulating this background.

[47] It might well be possible to design a tau *veto* algorithm that performs better than that used by DELPHES. We have not attempted to do so since at the end the SM background will be dominated by $Z \to \nu\bar{\nu}$ events even assuming DELPHES efficiencies.

[48] M. Martinez *et al.* (ATLAS Collaboration), EPJ Web Conf. **28**, 12015 (2012).

[49] S. Chatrchyan *et al.* (CMS Collaboration), arXiv:1206.5663.

[50] R. Barbieri and L. Maiani, Nucl. Phys. **B224**, 32 (1983); J. A. Grifols and J. Sola, Phys. Lett. **137B**, 257 (1984); C. S. Lim, T. Inami, and N. Sakai, Phys. Rev. D **29**, 1488 (1984); M. Drees and K. Hagiwara, Phys. Rev. D **42**, 1709 (1990).